Diisopropylfluorophosphate-induced status epilepticus drives complex glial cell phenotypes in adult male mice

Clémence Maupu, Julie Enderlin, Alexandre Igert, Myriam Oger, Stéphane Auvin, Rahma Hassan-Abdi, Nadia Soussi-Yanicostas, Xavier Brazzolotto, Florian Nachon, Grégory Dal Bo, et al.

Neurobiology of Disease 152 (2021) 105276

Contents lists available at ScienceDirect

Neurobiology of Disease

journal homepage: www.elsevier.com/locate/ynbdi

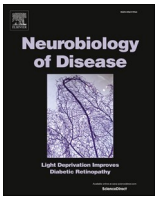

Diisopropylfluorophosphate-induced status epilepticus drives complex glial cell phenotypes in adult male mice

Clémence Maupu [a], Julie Enderlin [b,c], Alexandre Igert [a], Myriam Oger [d], Stéphane Auvin [b,c], Rahma Hassan-Abdi [b], Nadia Soussi-Yanicostas [b], Xavier Brazzolotto [a], Florian Nachon [a], Grégory Dal Bo [a], Nina Dupuis [a,*]

[a] Département de Toxicologie et risques chimiques, Institut de recherche biomédicale des armées, BP73, F-91223 Brétigny sur Orge cedex, France
[b] Université de Paris, NeuroDiderot, Inserm, F-75019 Paris, France
[c] Service de neurologie pédiatrique, AP-HP, Hôpital Robert Debré, F-75019 Paris, France
[d] Unité Imagerie, Institut de recherche biomédicale des armées, BP73, F-91223 Brétigny sur Orge cedex, France

ARTICLE INFO

Keywords:
Astrocyte
Microglia
Cytokines
Seizure
DFP
Organophosphates
Organophosphorus
SE
Mice

ABSTRACT

Organophosphate pesticides and nerve agents (OPs), are characterized by cholinesterase inhibition. In addition to severe peripheral symptoms, high doses of OPs can lead to seizures and status epilepticus (SE). Long lasting seizure activity and subsequent neurodegeneration promote neuroinflammation leading to profound pathological alterations of the brain.

The aim of this study was to characterize neuroinflammatory responses at key time points after SE induced by the OP, diisopropylfluorophosphate (DFP). Immunohistochemistry (IHC) analysis and RT-qPCR on cerebral tissue are often insufficient to identity and quantify precise neuroinflammatory alterations. To address these needs, we performed RT-qPCR quantification after whole brain magnetic-activated cell-sorting (MACS) of CD11B (microglia/infiltrated macrophages) and GLAST (astrocytes)-positive cells at 1, 4, 24 h and 3 days post-SE. In order to compare these results to those obtained by IHC, we performed, classical Iba1 (microglia/infiltrated macrophages) and GFAP (astrocytes) IHC analysis in parallel, focusing on the hippocampus, a brain region affected by seizure activity and neurodegeneration.

Shortly after SE (1–4 h), an increase in pro-inflammatory (M1-like) markers and A2-specific markers, proposed as neurotrophic, were observed in CD11B and GLAST-positive isolated cells, respectively. Microglial cells successively expressed immuno-regulatory (M2b-like) and anti-inflammatory (M2a-like) at 4 h and 24 h post-SE induction. At 24 h and 3 days, A1-specific markers, proposed as neurotoxic, were increased in isolated astrocytes. Although IHC analysis presented no modification in terms of percentage of marked area and cell number at 1 and 4 h after SE, at 24 h and 3 days after SE, microglial and astrocytic activation was visible by IHC as an increase in Iba1 and GFAP-positive area and Iba1-positive cells in DFP animals when compared to the control.

Our work identified sequential microglial and astrocytic phenotype activation. Although the role of each phenotype in SE cerebral outcomes requires further study, targeting specific markers at specific time point could be a beneficial strategy for DFP-induced SE treatment.

1. Introduction

Exposure to organophosphate pesticides and nerve agents (OPs) represents a threat for both civilian and military communities. In addition to severe peripheral symptoms, high doses of OPs can elicit seizures that rapidly progress into status epilepticus (SE). SE is a life-threatening neurological emergency characterized by continuous seizures without full recovery resulting in subsequent neuronal damage, cognitive alterations and epileptogenesis (Auvin and Dupuis, 2014). OPs act as potent irreversible inhibitors of both central and peripheral cholinesterases

Abbreviations: AChE, acetylcholinesterase; AS, atropine sulfate; CA1, cornu ammonis 1; CA3, cornu ammonis 3; ChEs, cholinesterases; DFP, Diisopropylfluorophosphate; DG, dentate gyrus; HI-6, asoxime; icv, intracerebroventricular; IHC, immunohistochemistry; ip, intraperitoneal; KA, kainate; OPs, organophosphate compounds; sc, subcutaneous; SE, status epilepticus; SRBD, seizure-related brain damage; WT, wild type.

* Corresponding author at: Institut de recherche biomédicale des armées, 1 Place Général Valérie André, BP 73, 91223 Brétigny sur Orge cedex, France.
E-mail address: ninadupuis@yahoo.fr (N. Dupuis).

https://doi.org/10.1016/j.nbd.2021.105276
Received 14 September 2020; Received in revised form 14 December 2020; Accepted 24 January 2021
Available online 30 January 2021

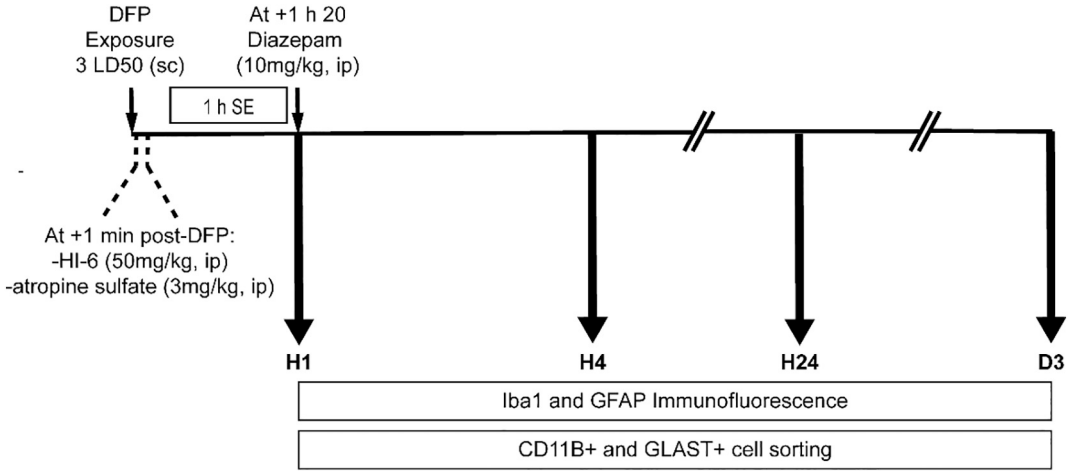

Fig. 1. DFP exposure protocol. Mice received an injection of DFP (3 LD50 = 9.93 mg/kg, LD50 calculated without HI-6 and AS post-treatment, 10 ml/kg, s.c.) followed by combined i.p. injection of HI-6 (50 mg/kg) and atropine sulfate (3 mg/kg) at +1 min of DFP injection. HI-6 and AS post-treatment is used to reduce respiratory distress and mortality. Except for the 1 h experimental group, all animals received Diazepam (10 mg/kg, i.p.), eighty minutes after DFP injection, corresponding to 1 h in SE. Control animals received all treatments after vehicle injection without DFP. Iba1 and GFAP immunofluorescence, and CD11B+ and GLAST+ cell sortings were conducted 1 h, 4 h, 24 h and 3 d post-DFP injection. ip, intraperitoneal; sc, subcutaneous.

(ChEs), resulting in uncontrolled activation of cholinergic receptors due to acetylcholine accumulation. In the central nervous system, excessive activation at muscarinic receptors by acetylcholine can initiate extended seizures (Hamilton et al., 1997) evolving to self-sustained SE with the additional involvement of glutamatergic and GABAergic systems imbalances. The first-line treatment of OP poisoning consists of injecting a muscarinic antagonist (*e.g.* atropine sulfate) combined with an oxime, which acts mainly as a peripheral ChE re-activator (*e.g.* pralidoxime or obidoxime). Additionally, the administration of an anticonvulsant (a benzodiazepine or a prodrug like avizafone) is currently indicated in the early phase of OP poisoning in order to control seizures and SE. However, experimental data in line with clinical experience clearly show that approximately 30–40 min after the initial seizures, SE becomes refractory to benzodiazepines and classical anti-epileptic drugs (Dhir et al., 2020; Mazarati et al., 1998; Bankstahl and Löscher, 2008; Kuruba et al., 1864; Wu et al., 2018; McDonough et al., 2010; Todorovic et al., 2012). In animal models, 30 min of unabated SE is also associated with severe seizure-related brain damage (Baille et al., 2005; Deshpande et al., 2016; Li et al., 2011; McDonough and Shih, 1997) and long-term consequences such as epilepsy and cognitive decline (Auvin and Dupuis, 2014).

Excitotoxic neuronal damage and seizure activity following SE development activate a neuroinflammatory response with marked microglia and astrocyte activation (Li et al., 2015; Rojas et al., 2015; Guignet et al., 2020; Sisó et al., 2017; Liu et al., 2012). Conversely, neuroinflammatory mechanisms have been implicated in SE-induced excitotoxic neuronal death, epileptogenesis and drug-resistance (Wu et al., 2018; Todorovic et al., 2012; Li et al., 2011; Rojas et al., 2015; Kadriu et al., 2009; Shrot et al., 2014). Reactive microglia and astrocytes can both have either protective or deleterious effects suggesting functional heterogeneity for both cell types. Based on *in vitro* experiments, microglia has been categorized into pro-inflammatory (M1-like), anti-inflammatory (M2a-like) and immuno-regulatory (M2b-like) subtypes (Chhor et al., 2013; Colton, 2009; Prinz et al., 2011). Likewise, reactive astrocytes have also been recently differentiated in A1 and A2 phenotypes (Liddelow et al., 2017a; Zamanian et al., 2012). Reactive astrocytes expressing A1 markers were described after neuroinflammation induced by lipopolysaccharide injection and are thought to confer neurotoxic effects. In contrast, A2 markers were described in astrocytes after ischemia and are thought to confer recovery and repair as they include many neurotrophic factors. Although the different subtypes are more likely a continuum with possibly numerous sub-classes, the different subtypes help our understanding of the complex neuroinflammatory mechanisms taking place after a neurological insult as SE.

We have recently developed and characterized a new convulsive mouse model of OP exposure using diisopropylfluorophosphate (DFP) (Enderlin et al., 2020). In this model, DFP induces electrographic SE within 20 min and all seizing animals develop long-lasting SE. To study neuroinflammation in this model, we choose 4 key time points: 1 h after DFP injection corresponding to the onset of benzodiazepine resistance, 4 h corresponding to beginning of neuronal suffering observed by the marker FluoroJade C, 24 h corresponding to the peak of neurodegeneration and 3 days corresponding to neurodegeneration and marked cerebral inflammation.

Here, we characterize changes in microglial activation state by isolating specific cellular populations using magnetic cell sorting from whole brains followed by RT-qPCR to identify sequential pro-inflammatory, immuno-modulatory and anti-inflammatory marker up-regulation beginning 1 h after DFP exposure. Using the same technique, we observed that A2 astrocyte marker up-regulation precedes the A1 marker up-regulation. In parallel, we show through histology that DFP-induced SE is associated with microglia and astrocyte activation in the hippocampus. In this study, we focus on the hippocampal formation, given its crucial role in seizure development and epileptogenesis. These data can help understand microglial and astrocytic activation kinetics and adapt treatment paradigms in order to address the different phases of neuroinflammation and increase therapeutic impact.

2. Material and methods

2.1. Animals

Adult male Swiss mice (8 weeks, Janvier Labs, Le Genest-Saint-Isle, France) were housed four per cage with a 12 h/12 h light/dark cycle and food and water *ad libitum*. A period of 5–7 days of acclimation to housing conditions was observed. All animals were 9 weeks old when exposed to DFP.

All experiments involving animals complied with the ARRIVE guidelines and were performed in accordance with EU Directive 2010/63/EU for animal experiments following protocols approved by the ethics committee according to applicable French legislation, in compliance with the "3Rs" policy of reduction, refinement and replacement of animal use for scientific procedures (Directive 2010/63/UE, décret 2013–118, approval number 9642–2017040316305252).

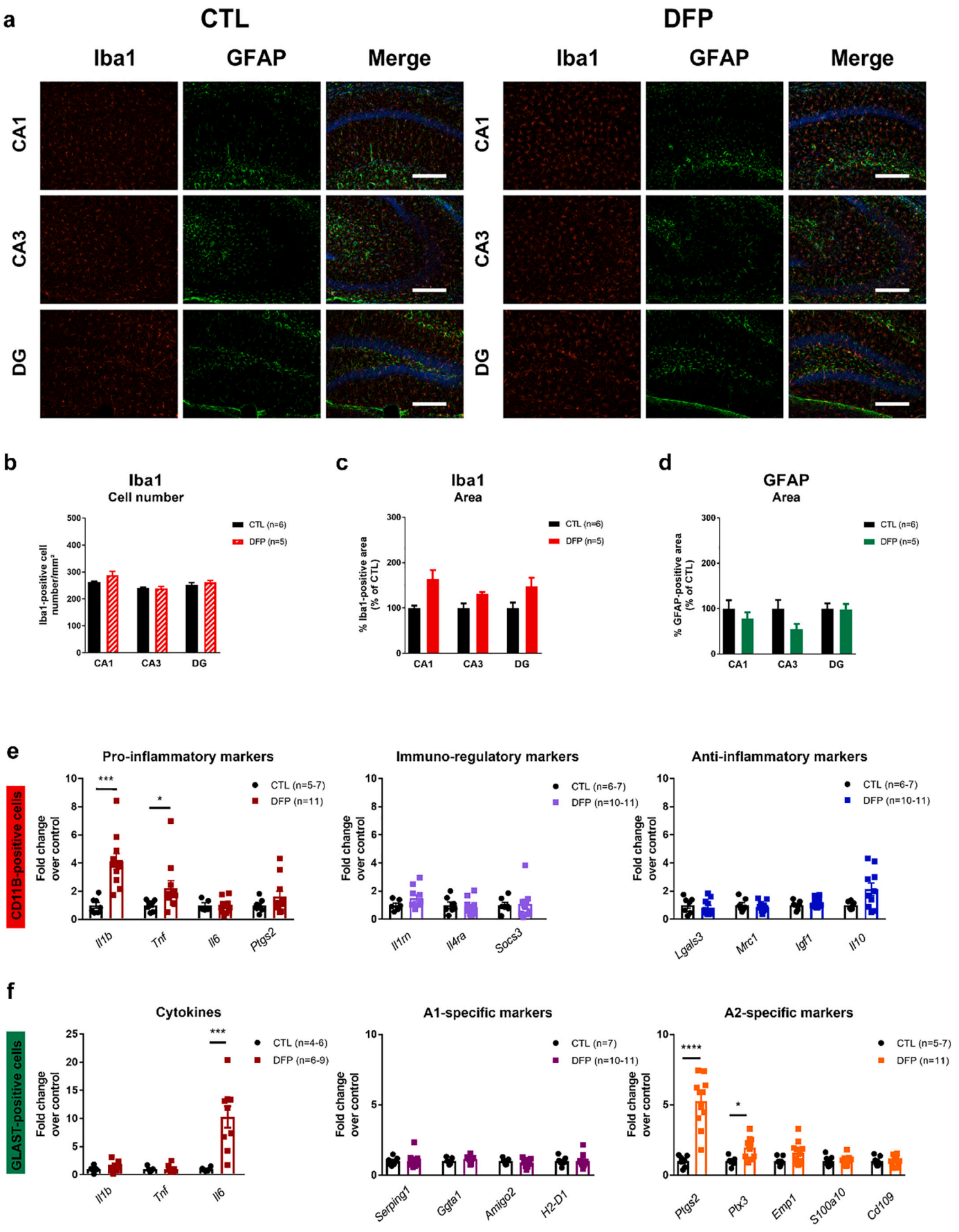

(caption on next page)

Fig. 2. Neuroinflammatory response 1 h after DFP exposure. a Immunohistochemical detection of the microglial/macrophage marker Iba1 (*red*) and the astrocytic marker GFAP (*green*) in CA1, CA3 and DG hippocampal regions of control (CTL) and DFP SE mice. **b** Iba1-positive cell number, **c** Iba1-postitive area and **d** GFAP-positive area in in CA1, CA3 and DG hippocampal regions of control (CTL) and DFP SE mice. **e** Quantitative RT-PCR analysis of pro-inflammatory (*Il1b, Tnf, Il6, Ptgs2*), immuno-regulatory (*Il1rn, Il4ra, Socs3*) and anti-inflammatory (*Lgals3, Mrc1, Igf1, Il10*) markers in isolated CD11B-positive cells of control (CTL) and DFP SE brains. Quantitative RT-PCR analysis of cytokines (*Il1b, Tnf, Il6*), A1-associated reactive (*Serping1, Ggta1, Amigo2, H2-D1*) and A2-associated reactive (*Ptgs2, Ptx3, Emp1, S100a10, Cd109*) markers in isolated GLAST-positive cells of control (CTL) and DFP SE brains. $*p < 0.05$, $**p < 0.01$, $***p < 0.001$, $****p < 0.0001$ *vs* CTL (Mann-Whitney test). Data are presented as mean ± SEM. Scale bar = 200 μm.

2.2. Drugs

DFP (Sigma Aldrich, L'Isle d'Abeau Chesnes, France) was freshly prepared by diluting a concentrated solution (0,1 g/ml in isopropanol) in 0.9% (*w/v*) ice-cold saline. The oxime HI-6 (1–2-hydroxy-iminomethyl-1-pyridino-2-oxanopropane) dichloride was a generous gift of DRDC Suffield (Canada). Atropine sulfate (AS, Sigma Aldrich, L'Isle d'Abeau Chesnes, France) and HI-6 were diluted in 0.9% (*w/v*) saline. Veterinary Diazepam (TVM, Lempdes, France) was used undiluted.

2.3. DFP exposure

The day of the experiment, mice received an injection of DFP (3 LD50 = 9.93 mg/kg, LD50 calculated without HI-6 and AS post-treatment, 10 ml/kg, s.c.) followed by combined i.p. injection of HI-6 (50 mg/kg) and AS (3 mg/kg) at +1 min of DFP injection. HI-6 and AS post-treatment is used to reduce respiratory distress and mortality. As previously shown (Enderlin et al., 2020), the OP exposure protocol used in this project caused reduced mortality. In this project, the mortality rate in the DFP treated animals was <10%, death occurring in the first 30 min after DFP injection. The protocol used for drugs administration is depicted in Fig. 1.

Except for the 1 h experimental group, all animals received Diazepam (10 mg/kg, i.p.), eighty minutes after DFP injection, corresponding to 1 h in SE. Diazepam was used to minimize the impact of SE on animal welfare. Control animals received all treatments after vehicle injection without DFP.

Based on our previous work using electrocorticography (ECoG) and behavioral characterization of seizures, we validated specific symptoms of electrographic epileptic seizures (head and forelimb clonus, evaluated 1 h after DFP injection) (Enderlin et al., 2020). To avoid the neuroinflammatory response induced by ECoG electrodes surgery, in this work we evaluated behavioral signs of seizures to distinguished animals with and without SE.

2.4. Immunofluorescence

After deep anesthesia, animals were transcardially perfused with 10 ml of 0.9% NaCl/5 UI/ml heparin, followed by 50 ml of 4% paraformaldehyde (PFA) in phosphate buffer. After overnight post-fixation in 4% PFA, brains were cryoprotected 24 h in 30% sucrose and then frozen 1 min in −40 °C isopentane. Thirty μm-thick coronal sections were immunolabeled with anti-Iba1 (1:1000, Wako) and anti-GFAP (1:1000, Millipore) antibodies overnight at room temperature. Brain sections were then washed in PBS and subsequently incubated for 1 h at room temperature in 1:500 Alexa Fluor 555 anti-rabbit IgG and 1:500 Alexa Fluor 488 anti-mouse IgG (Invitrogen).

For each animal, analyses were conducted on images acquired at 3 rostrocaudal levels each separated by 180 μm centered on fig. 48 of Franklin and Paxinos mouse brain atlas (3rd edition). For each image, using Fiji software, regions of interest were delimited in the CA1, CA3 and dentate gyrus hippocampal regions. The same regions of interest were used for Iba1 cell counting and Iba1 and GFAP % of positive area evaluation. The final results were expressed as % of positive area and % of mean control values for Iba1 and GFAP % of positive area and in cell number/mm^2 for Iba1 cell counts.

2.5. Neural tissue dissociation and magnetic activated cell sorting

Brains were collected (1 animal per sorting) for cell dissociation and microglial cells and astrocytes were enriched using a magnetic-bead-coupled antibody (anti-CD11B and anti-GLAST respectively) extraction technique (MACS), as previously described and according to the manufacturer's protocol ((Rideau Batista Novais et al., 2016); Miltenyi Biotec, Bergisch Gladbach, Germany). In brief, after removing the cerebellum and olfactory bulbs, each brain was dissociated using the adult brain dissociation kit. From the resulting brain homogenates, microglial cells were enriched by MACS using anti-CD11B microbeads. After elution, isolated cells were centrifuged for 10 min at 300*g* and conserved at −80 °C. Astrocytes were enriched by MACS using anti-GLAST microbeads on the remaining cells and collected similarly to microglial cells. Microglial cells and astrocytes were sorted 1 h, 4 h, 24 h and 3 d after vehicle/DFP injection in control (n = 7–8 /time point) and DFP (n = 12–16/time point) mice.

2.6. RNA extraction and RT-qPCR

Total RNA from isolated microglial cells and astrocytes were extracted with NucleoSpin ® RNA Plus XS kit according to the manufacturer's instructions (Macherey-Nagel, Hoerdt, France). Purified RNA quality and concentration were assessed by spectrophotometry using a NanoDropTM (Thermoscientific, Wilmington, DE). 200–400 ng of total RNA was subjected to reverse transcription using the IscriptTM cDNA synthesis kit (Bio-Rad, Marnes-la-Coquette, France). RT-qPCR was performed in triplicate for each sample on a CFX384 Real Time System (Bio-Rad), using the SYBR Green Supermix (Bio-Rad) for 40 cycles. Amplification specificity was assessed by melting curve analysis. Primers were designed using Primer3 software and manufactured by Eurofins Genomics (Ebersberg, Germany). Primer sequences are summarized in Table S1. For expression analyses of CD11B-positive cells, for each sample, the expression of genes of interest was calculated relative to the expression of the reference gene TATA-box binding protein (*Tbp*). For expression analyses of GLAST-positive cells, for each sample, the expression of genes of interest was calculated relative to the expression of the reference gene ribosomal protein L13a (*Rpl13a*). The final results are presented as fold change over control mean values. Analyses were performed using Bio-Rad CFX Manager 3.0.

2.7. Statistical analysis

Data were analyzed using PRISM 7 software (GraphPad, San Diego, CA, U.S.A.). Data were expressed as means ± standard errors of the mean (SEM). Statistical comparison to control group was performed using the Mann-Whitney test. Sample sizes are indicated in the figures.

3. Results

3.1. Microglial and astrocytic activation 1 h after DFP exposure

To determine glial activation state at the time of SE drug refractoriness, we quantified microglial and astrocytic activations 1 h after DFP exposure, corresponding to 40 min of SE according to our previous report (Enderlin et al., 2020).

We first studied microglial and astrocytic activation using expression analysis of markers of polarized states. Gene expression analysis was

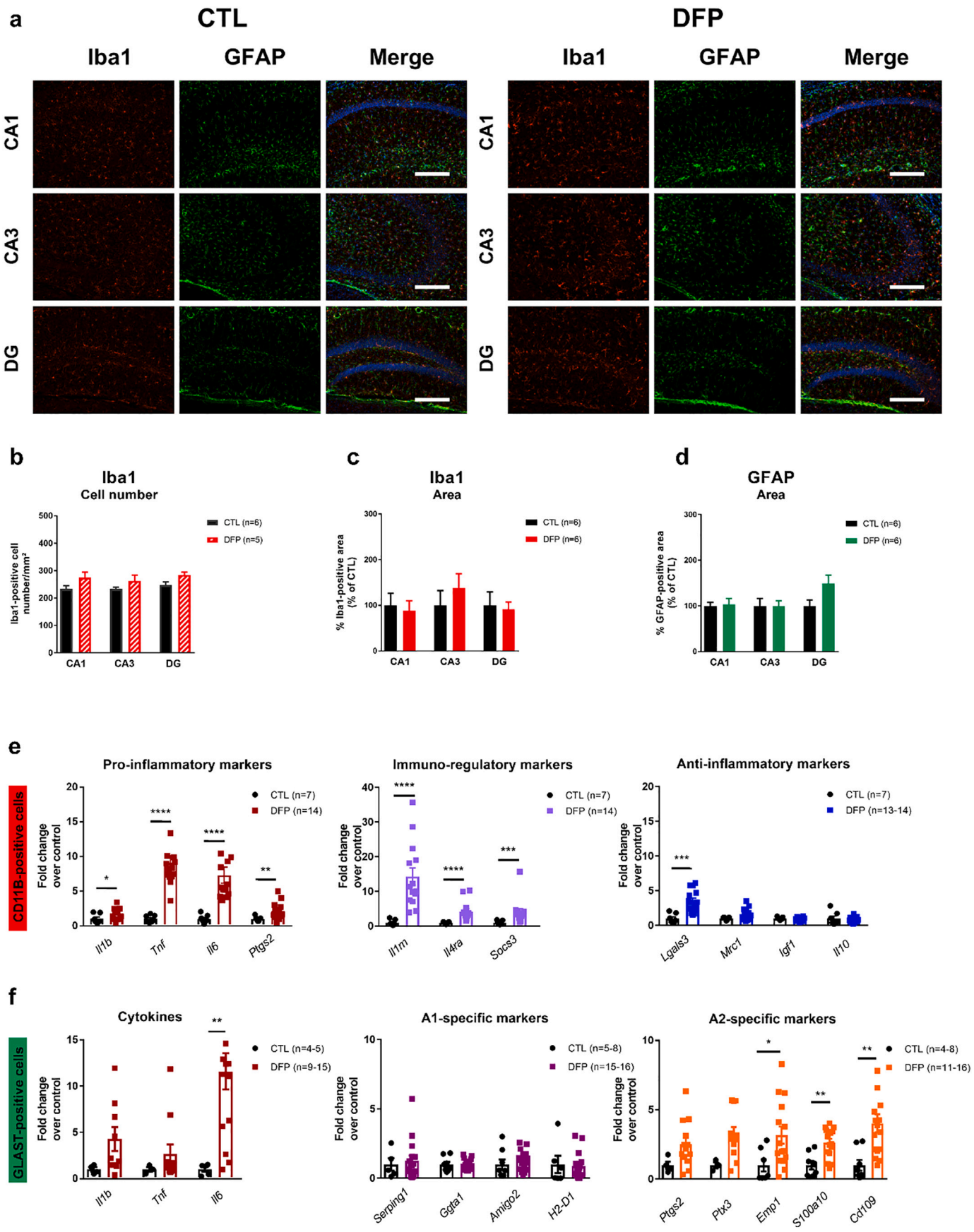

(caption on next page)

Fig. 3. Neuroinflammatory response 4 h after DFP exposure. a Immunohistochemical detection of the microglial/macrophage marker Iba1 (*red*) and the astrocytic marker GFAP (*green*) in CA1, CA3 and DG hippocampal regions of control (CTL) and DFP SE mice. **b** Iba1-positive cell number, **c** Iba1-postitive area and **d** GFAP-positive area in in CA1, CA3 and DG hippocampal regions of control (CTL) and DFP SE mice. **e** Quantitative RT-PCR analysis of pro-inflammatory (*Il1b, Tnf, Il6, Ptgs2*), immuno-regulatory (*Il1rn, Il4ra, Socs3*) and anti-inflammatory (*Lgals3, Mrc1, Igf1, Il10*) markers in isolated CD11B-positive cells of control (CTL) and DFP SE brains. Quantitative RT-PCR analysis of cytokines (*Il1b, Tnf, Il6*), A1-associated reactive (*Serping1, Ggta1, Amigo2, H2-D1*) and A2-associated reactive (*Ptgs2, Ptx3, Emp1, S100a10, Cd109*) markers in isolated GLAST-positive cells of control (CTL) and DFP SE brains. $*p < 0.05$, $**p < 0.01$, $***p < 0.001$, $****p < 0.0001$ *vs* CTL (Mann-Whitney test). Data are presented as mean ± SEM. Scale bar = 200 μm.

performed after CD11B-positive (microglia/infiltrating macrophages) and GLAST-positive (astrocytes) cell sorting in DFP SE and control whole brains. In isolated CD11B-positive cells, quantitative RT-PCR experiments showed a differential increase of pro-inflammatory markers (*Il1b, Tnf*) but lack of immuno-regulatory (*Il1rn, Il4ra, Socs3*) and anti-inflammatory markers (*Lgals3, Mrc1, Igf1, Il10*) modulations (Fig. 2e). In GLAST-positive cells, quantitative RT-PCR experiments indicated an increase of A2-specific markers *Ptgs2* and *Ptx3*, as well as *Il6* cytokine mRNA but no A1-specific marker (*Serping1, Ggta1, Amigo2, H2-D1*) modifications (Fig. 2f).

Our immunohistochemical (IHC) analysis of Iba1-positive microglia/infiltrated macrophages and GFAP-positive astrocytes focused on the three main regions of the hippocampus, Cornu Ammonis-1 (CA1), Cornu Ammonis-3 (CA3) and the dentate gyrus (DG), which are particularly sensitive to OP poisoning (Flannery et al., 2016; Qiao et al., 2004). Receiving input from the entorhinal cortex, the DG, CA3 and CA1 are part of the excitatory loop, completed by inhibitory neurons, implicated in memory processes, as well as, susceptibility to seizures and neurodegeneration. In our previous work, we showed that these three regions were affected by neuronal activation and neurodegeneration (Enderlin et al., 2020). One hour after DFP injection, Iba1-positive cell number and Iba1-positive area were not statistically different in DFP SE animals when compared to control animals in CA1, CA3 and DG (Fig. 2a–c). In the same animals, GFAP–positive area was also unaltered by SE (Fig. 2a and d). Given the intertwining of astrocyte processes, we were unable to quantify GFAP-positive cell numbers at any time point.

Taken together, these findings indicate that 1 h after DFP injection, microglial cells very rapidly develop an activated state with a pro-inflammatory phenotype. Interestingly, at the same time, expression experiments on isolated astrocytes, allowed us to observe that they do not yet develop a neurotoxic A1-associated reactivity but an A2-associated reactivity associated with an *Il6* mRNA up-regulation. This is supported by the lack of pro-inflammatory cytokines *Ilb* and *Tnf* mRNA up-regulation in GLAST-positive cells.

3.2. Microglial and astrocytic activation 4 h after DFP exposure

Going forward, we next studied microglial and astrocytic activation 4 h after DFP injection.

At this time point, RNA expression analysis identified a combined pro-inflammatory and immuno-regulatory marker up-regulation in CD11B-positive microglia/infiltrated macrophages, associated with an increase of the anti-inflammatory marker, *Lgals3* (Fig. 3e). At the same time, isolated GLAST-positive astrocytes developed a clear A2-associated phenotype with the up-regulation of *Emp1*, *S100a10* and *Cd109* A2-specific markers (Fig. 3f). As with the 1 h time point, this A2 activation state was associated with *Il6* mRNA increase. No A1-specific markers were modified, nor *Il1b* and *Tnf* mRNA (Fig. 3f).

The IHC analysis of the hippocampus showed no modifications of Iba1-positive cell numbers and Iba1-positive area (Fig. 3a–c). Similarly, GFAP-positive area was not different in DFP SE animals compared to control animals (Fig. 3a and d).

These findings indicate that 4 h after DFP injection, microglia develop in parallel a pro-inflammatory phenotype and an immuno-regulatory phenotype. These experiments could not evaluate if these 2 activated states were present in the same microglial population or in 2 different cell populations. At the same time point, the astrocytic activation state did not change from the 1 h time point, though they strengthened their A2 phenotype associated with an *Il6* mRNA up-regulation. Interestingly, the A1 phenotype was also not observed at this time point.

3.3. Microglial and astrocytic activation 24 h after DFP exposure

We have previously reported important neurodegeneration 24 h after DFP-induced SE (Enderlin et al., 2020). At this time point, CA1, CA3 and DG hippocampal regions, as with other brain regions, are affected by prominent neuronal damage.

At 24 h post-DFP exposure, isolated CD11B-positive microglia/infiltrated macrophages presented the 3 microglial activation phenotypes: pro-inflammatory, immuno-regulatory and newly up-regulated anti-inflammatory as seen with up-regulated *Lgals3* and *Mrc1* (Fig. 4e). Likewise, isolated GLAST-positive astrocytes developed different activation phenotypes. Both A1-specific markers (*Serping1*, *Ggta1*, *H2-D1)* and A2-specific markers (*Ptx3*, *Emp1*, *S100a10*, *Cd109*) were up-regulated (Fig. 4f). These astrocytic activation states were associated with prominent *Il6* up-regulation and no significant increase of *Il1b* and *Tnf* transcripts levels in DFP SE animals compared to control animals (Fig. 4f).

The IHC analysis of the hippocampus uncovered an increase in Iba1 microglia/infiltrated macrophage cell numbers (Fig. 4a and b), as well as, an important increase in Iba1-positive area in the CA1 and CA3 hippocampal regions (Fig. 4a and c). In these 2 regions, GFAP-positive area was also increased (Fig. 4a and d). Conversely, though also affected by brain damage at this time point (Enderlin et al., 2020), the DG region presented no elevation of Iba1, nor GFAP-positive area.

These results indicate important neuroinflammatory activations 24 h after DFP-induced SE. Microglial cells present pro-inflammatory, immuno-regulatory and anti-inflammatory phenotypes. At the same time point, astrocytes present 2 types of activations states: A1 and A2 activation states with joint *Il6* mRNA up-regulation.

3.4. Microglial and astrocytic activation 3 days after DFP exposure

We next studied microglial and astrocytic activation 3 days after DFP-induced SE. This time point has been widely described by others using IHC techniques (Wu et al., 2018; Sisó et al., 2017; Liu et al., 2012).

Quantitative RT-PCR experiments indicated marked activation of CD11B-positive isolated microglia/infiltrated macrophages. As with the 24 h time point, these cells developed 3 activation states with an increase of pro-inflammatory, immuno-regulatory and anti-inflammatory markers (Fig. 5e). Unlike the other genes, *Mrc1* was down-regulated in DFP SE animals compared to control animals (Fig. 5e). In parallel, GLAST-positive astrocytes maintained their A1 and A2-associated activation states. These 2 activation states were, however, not associated with an increase in *Il1b*, *Tnf* or *Il6* mRNA in DFP SE animals compared to control animals (Fig. 5f). Overall, we observed that cytokines expression seemed more variable in DFP SE animals in astrocytes compared to microglia.

IHC evaluation of neuroinflammation in the hippocampus revealed marked Iba1-positive cell number increase in the 3 hippocampal regions studied (Fig. 5a and b). This was associated with an increase of Iba1-positive area in the CA3 and DG (Fig. 5a and c). Massive increase of GFAP-positive area was also visible in the 3 hippocampal regions (Fig. 5a and d).

Taken together, these findings show pronounced microglial and

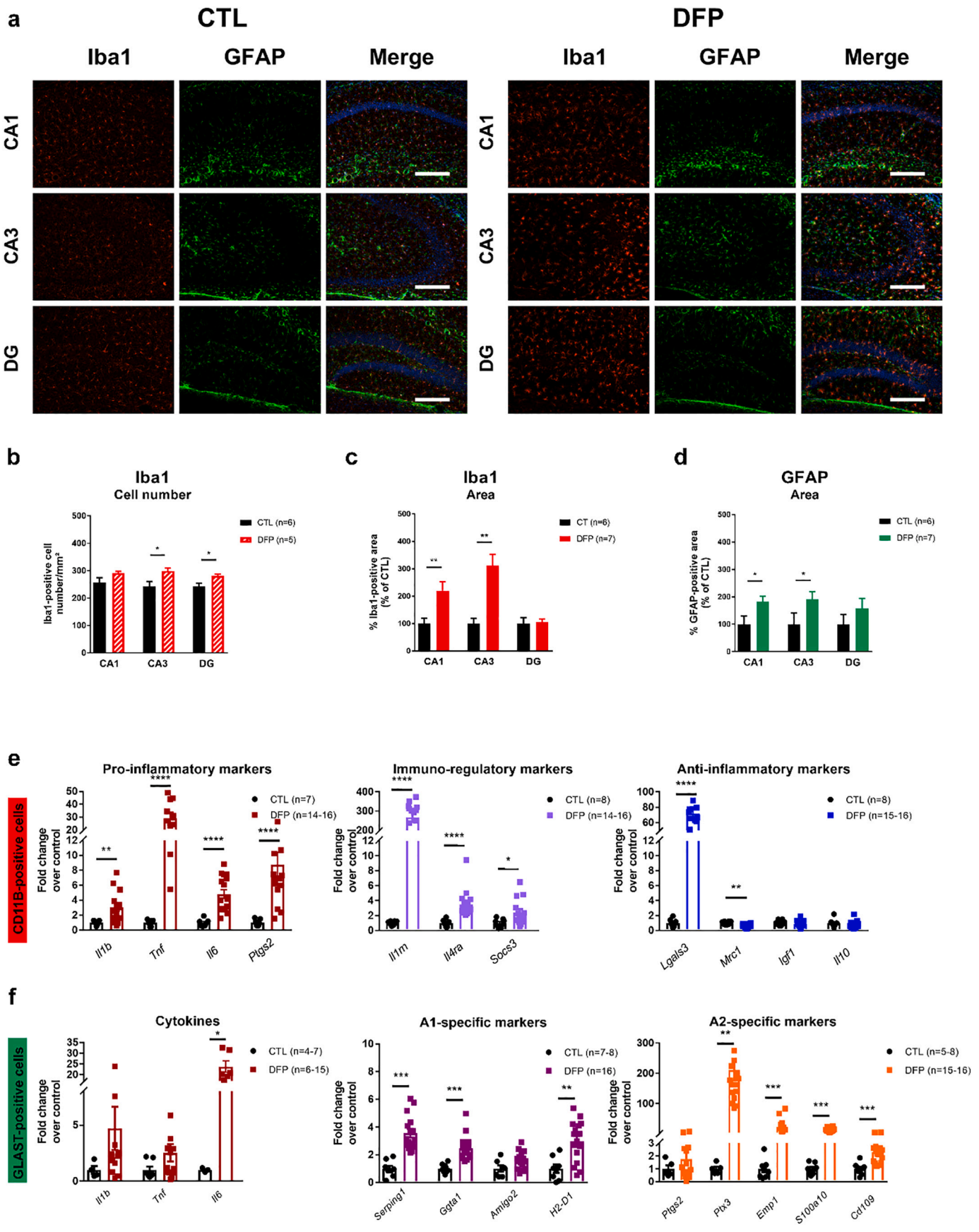

(caption on next page)

Fig. 4. Neuroinflammatory response 24 h after DFP exposure. a Immunohistochemical detection of the microglial/macrophage marker Iba1 (*red*) and the astrocytic marker GFAP (*green*) in CA1, CA3 and DG hippocampal regions of control (CTL) and DFP SE mice. **b** Iba1-positive cell number, **c** Iba1-postitive area and **d** GFAP-positive area in in CA1, CA3 and DG hippocampal regions of control (CTL) and DFP SE mice. **e** Quantitative RT-PCR analysis of pro-inflammatory (*Il1b, Tnf, Il6, Ptgs2*), immuno-regulatory (*Il1rn, Il4ra, Socs3*) and anti-inflammatory (*Lgals3, Mrc1, Igf1, Il10*) markers in isolated CD11B-positive cells of control (CTL) and DFP SE brains. Quantitative RT-PCR analysis of cytokines (*Il1b, Tnf, Il6*), A1-associated reactive (*Serping1, Ggta1, Amigo2, H2-D1*) and A2-associated reactive (*Ptgs2, Ptx3, Emp1, S100a10, Cd109*) markers in isolated GLAST-positive cells of control (CTL) and DFP SE brains. $*p < 0.05$, $**p < 0.01$, $***p < 0.001$, $****p < 0.0001$ *vs* CTL (Mann-Whitney test). Data are presented as mean ± SEM. Scale bar = 200 μm.

astrocytes activation 3 days after DFP-induced SE. At this time point, the DG is particularly affected by both activated cell types. All described markers are present with an up-regulation of pro-inflammatory, immune-regulatory and anti-inflammatory markers in CD11B-positive cells and A1 and A2-associated reactive markers in GLAST-positive astrocytes.

4. Discussion

Long lasting seizure activity and neurodegeneration induced by high doses of OPs promote neuroinflammation, which leads to profound pathological alterations of the brain (Todorovic et al., 2012; Deshpande et al., 2016; McDonough and Shih, 1997; Enderlin et al., 2020; de Araujo et al., 2012). Here, we characterized neuroinflammatory responses at key time points after DFP-induced SE. Using cell sorting, we conducted RT-qPCR experiments in order to decipher microglial and astrocytic reactive marker expression and extend our understanding of SE-related neuroinflammation. Compared to RT-qPCR on cerebral tissue, RT-qPCR after cell sorting allow us to identify the cellular origin of inflammatory gene up-regulation and confers increased sensitivity by concentrating on a specific cell type. Discussions on the existence of differential M1 and M2 phenotypes in microglial cells is still ongoing and the M1/M2 dichotomy is most certainly an oversimplification (Chu et al., 2019; Liu et al., 2018; Yuan et al., 2019; Ransohoff, 2016). However diverse opposing impacts of activated microglia on neuronal damage have been demonstrated and modulation of microglial cells polarization towards a M2 phenotype have been described as beneficial (Chu et al., 2019; Liu et al., 2018; Xu et al., 2017; Kong et al., 2016; Li et al., 1657). Based on differential molecular marker expressions, reactive astrocytes have also been subdivided in A1 and A2 (Liddelow et al., 2017a). A1 astrocytes that lose most normal astrocytic functions and gain neurotoxic function are associated with multiple human and experimental models of neurological insult (Liu et al., 2012; Aronica et al., 2012; Aronica and Crino, 2011; Steinhäuser and Seifert, 2012; Vezzani et al., 2008; Sofroniew and Vinters, 2010). Originally described after ischemia and postulated to be beneficial as they were associated with up-regulation of many neurotrophic factors, the impact of A2 astrocytes upon neuroinflammatory injury is mostly unclear (Liddelow et al., 2017a; Zamanian et al., 2012). It appears that both microglia and astrocyte polarizations are greatly dependent on the type of insult and the delay after the initial insult. Our current understanding of microglia polarization after SE is limited and astrocyte polarization has yet not been studied. Our study reveals sequential activation of microglial and astrocytic phenotypes.

As soon as 1 h post DFP injection, corresponding to 40 min of SE (Enderlin et al., 2020), we observe an early pro-inflammatory phenotype in microglia. Previous studies demonstrated that 30–40 min of DFP-induced SE was associated with benzodiazepine-refractoriness in rats (Kuruba et al., 1864; Wu et al., 2018; McDonough et al., 2010; Todorovic et al., 2012). In a different SE model, induced by intrahippocampal injection of KA, it has been shown that the pro-inflammatory cytokine IL1β could play an important role in benzodiazepine response in SE as IL1β icv injection prolonged diazepam latency to terminate SE (Xu et al., 2016). Furthermore, in this project, SE was responsive to diazepam at 40 min in *Il1r1* knock-out mice compared to WT mice (Xu et al., 2016). Our results show that, at this very early stage, *Il1b* mRNA increase is associated with microglia. At the same stage, neurotoxic A1 astrocytic activation is still absent, in accordance with the idea that pro-inflammatory microglia activation precedes pro-inflammatory astrocyte activation (Liddelow et al., 2017a). However, at the same time point, we observed an A2-associated reactive phenotype with the up-regulation of *Ptgs2*, coding for Cox2 protein, and *Ptx3* mRNA. Our results further show that this up-regulation of A2-associated markers is concomitant to an *Il6* increase. Expression of Il6 protein has been described in astrocytes 12 and 24 h after soman-induced SE in rats, but Il6 presence has not been studied at earlier stages (Johnson and Kan, 2010). IL6 is a pleiotropic cytokine, modulating the inflammatory response by exerting both protective and detrimental activities in neuronal tissue. Il6 icv injection has been shown to induce epileptogenesis with the occurrence of cortical seizures detected 3 days after the injection, in a dose-dependent manner, in C57Bl6 mice (Levy et al., 2015). Although A2 astrocytes are thought to be beneficial, A2 astrocytes expressing Cox2 have been proposed as deleterious on oligodendrocyte progenitor cell maturation in a mouse model of neonatal white matter injury (Shiow et al., 2017). Overall, we described for the first time the early A2 activation phenotype of astrocytes after SE. Its implication in SE maintenance and neuronal degeneration has to be further assessed.

Using the same techniques 4 h after DFP injection, no modifications were noticeable by IHC, however we observed an up-regulation of pro-inflammatory and immuno-regulatory markers in microglial cells. Interestingly, this time point is associated with a significant increase of *Il1rn* mRNA, which will persist for up to 3 days post-injection, with a ~270 fold increase at 24 h (Table 1). IL1RA protein, encoded by *IL1RN*, binds the receptor IL1R1 and blocks IL1α and IL1β signaling. IL1β-IL1R1 signaling has been widely implicated in seizure occurrence and epileptogenesis (for review, (Vezzani et al., 2011; van Vliet et al., 2018; Vezzani et al., 2019)) and an IL1β-IL1R1 signaling blockade has been shown to reduce seizure number, neurodegeneration, and epileptogenesis (Vezzani et al., 2010; Maroso et al., 2010; Iori et al., 2017; Noe et al., 2013; Vezzani et al., 2000). In this regard, soman-induced SE was accompanied with a mild increase of neurodegeneration in *Il1r1* and *Il1rn* knock-out mice but SE duration and severity have not been studied by EEG (Ferrara-Bowens et al., 2017). We did not observe *Il1b* mRNA up-regulation in isolated astrocytes at any time point. This is in accordance with the exclusive expression of Il1β at a protein level in activated microglia 24 h after soman-induced SE (Johnson and Kan, 2010). Astrocytic expression of Il1β is observed later in time from 4 days (Vinet et al., 2016) in pilocarpine SE model, but discrepancies exist as Il1β has been observed in astrocytes earlier in the pilocarpine model by others (Ravizza et al., 2008a) or in other types of seizures (Balosso et al., 2008; Akin et al., 2011; Ravizza et al., 2008b).

At 24 h after DFP-induced SE, in accordance with the massive neurodegeneration observed in our model (Enderlin et al., 2020), both microglial and astrocytic activation was visualized by IHC. In CD11B-positive isolated cells, while pro-inflammatory and immuno-regulatory markers were maintained, anti-inflammatory markers appeared up-regulated. This time point was associated with a ~72 fold increase of the *Lgals3* mRNA, which persisted 3 days post-SE (Table 1). Galectin-3 protein, encoded by *Lgals3*, released by microglia, plays a pivotal role in phagocytosis by binding targeted cells or bacteria (Cockram et al., 2019). Galectin-3-positive microglia were observed to engulf degenerative neurons in a model of ischemia by middle cerebral artery occlusion (Akin et al., 2011). Furthermore, in this model, *Lgals3* knock-out mice presented increased cell death, suggesting a protective role of Galectin-3 after ischemia (Lalancette-Hébert et al., 2012). Although, *Lgals3* mRNA is strongly up-regulated in microglia after pilocarpine-induced SE,

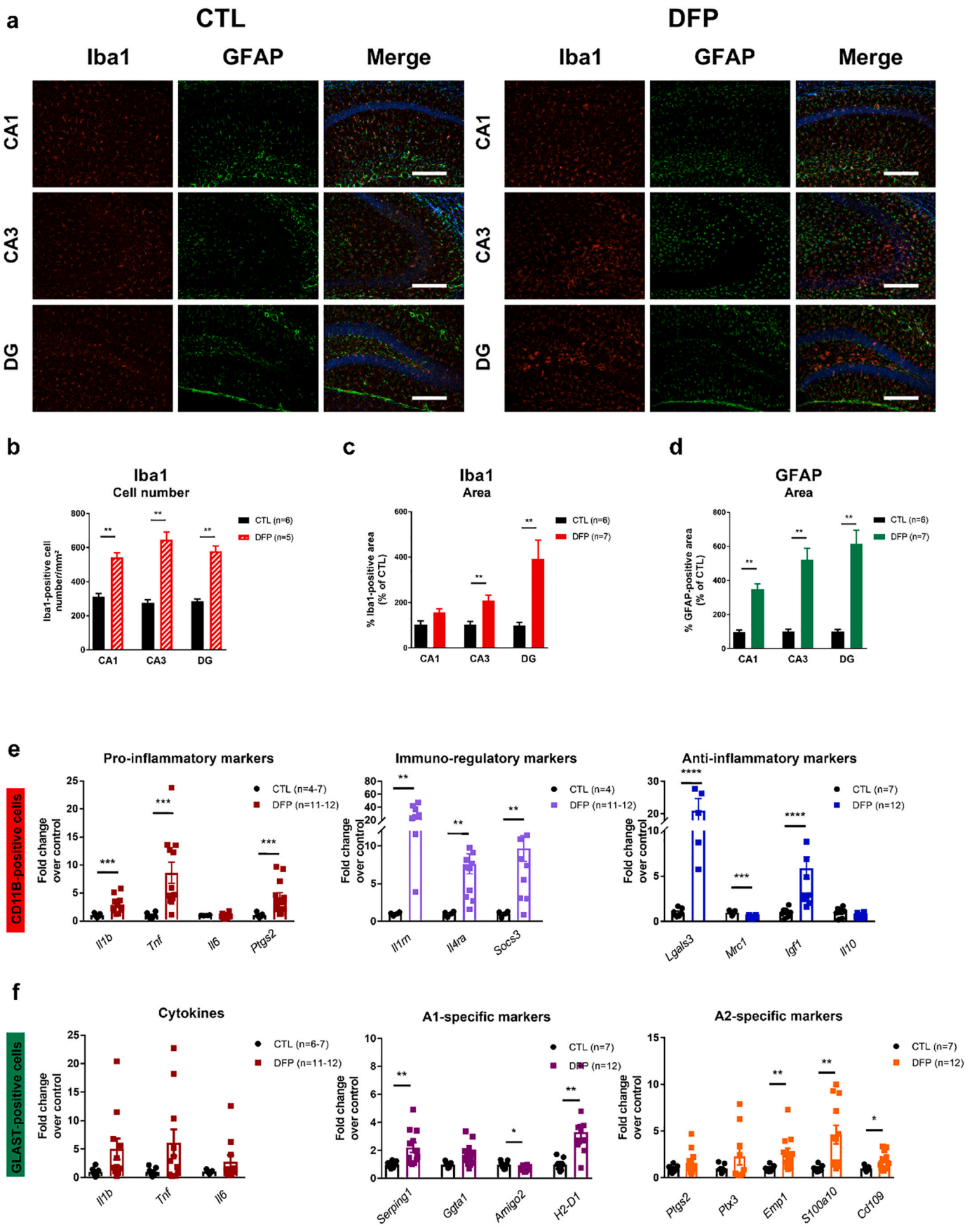

(caption on next page)

Fig. 5. Neuroinflammatory response 3 days after DFP exposure. a Immunohistochemical detection of the microglial/macrophage marker Iba1 (*red*) and the astrocytic marker GFAP (*green*) in CA1, CA3 and DG hippocampal regions of control (CTL) and DFP SE mice. **b** Iba1-positive cell number, **c** Iba1-postitive area and **d** GFAP-positive area in in CA1, CA3 and DG hippocampal regions of control (CTL) and DFP SE mice. **e** Quantitative RT-PCR analysis of pro-inflammatory (*Il1b, Tnf, Il6, Ptgs2*), immuno-regulatory (*Il1rn, Il4ra, Socs3*) and anti-inflammatory (*Lgals3, Mrc1, Igf1, Il10*) markers in isolated CD11B-positive cells of control (CTL) and DFP SE brains. Quantitative RT-PCR analysis of cytokines (*Il1b, Tnf, Il6*), A1-associated reactive (*Serping1, Ggta1, Amigo2, H2-D1*) and A2-associated reactive (*Ptgs2, Ptx3, Emp1, S100a10, Cd109*) markers in isolated GLAST-positive cells of control (CTL) and DFP SE brains. $*p < 0.05$, $**p < 0.01$, $***p < 0.001$, $****p < 0.0001$ *vs* CTL (Mann-Whitney test). Data are presented as mean ± SEM. Scale bar = 200 μm.

Table 1

Summary table of DFP-induced SE impact on neuroinflammation response compared to control group. For RT-qPCR analysis, light red and light green, fold change relative to controls: [2–5[; medium red and medium green, fold change relative to controls [5–10[; dark red and dark green, fold change relative to controls [10−300]; light blue fold change relative to controls [0.5–0.2[. For immunohistochemistry analysis, light red and light green, fold change relative to controls: [1.2–2[; medium red and medium green, fold change relative to controls [2–3[; dark red and dark green, fold change relative to controls (Dhir et al., 2020; Mazarati et al., 1998; Bankstahl and Löscher, 2008; Kuruba et al., 1864; Wu et al., 2018; McDonough et al., 2010; Todorovic et al., 2012; Baille et al., 2005); light blue fold change relative to controls [0.8–0.5[. $*p < 0.05$, $**p < 0.01$, $***p < 0.001$, $****p < 0.0001$ *vs* CTL (Mann-Whitney test).

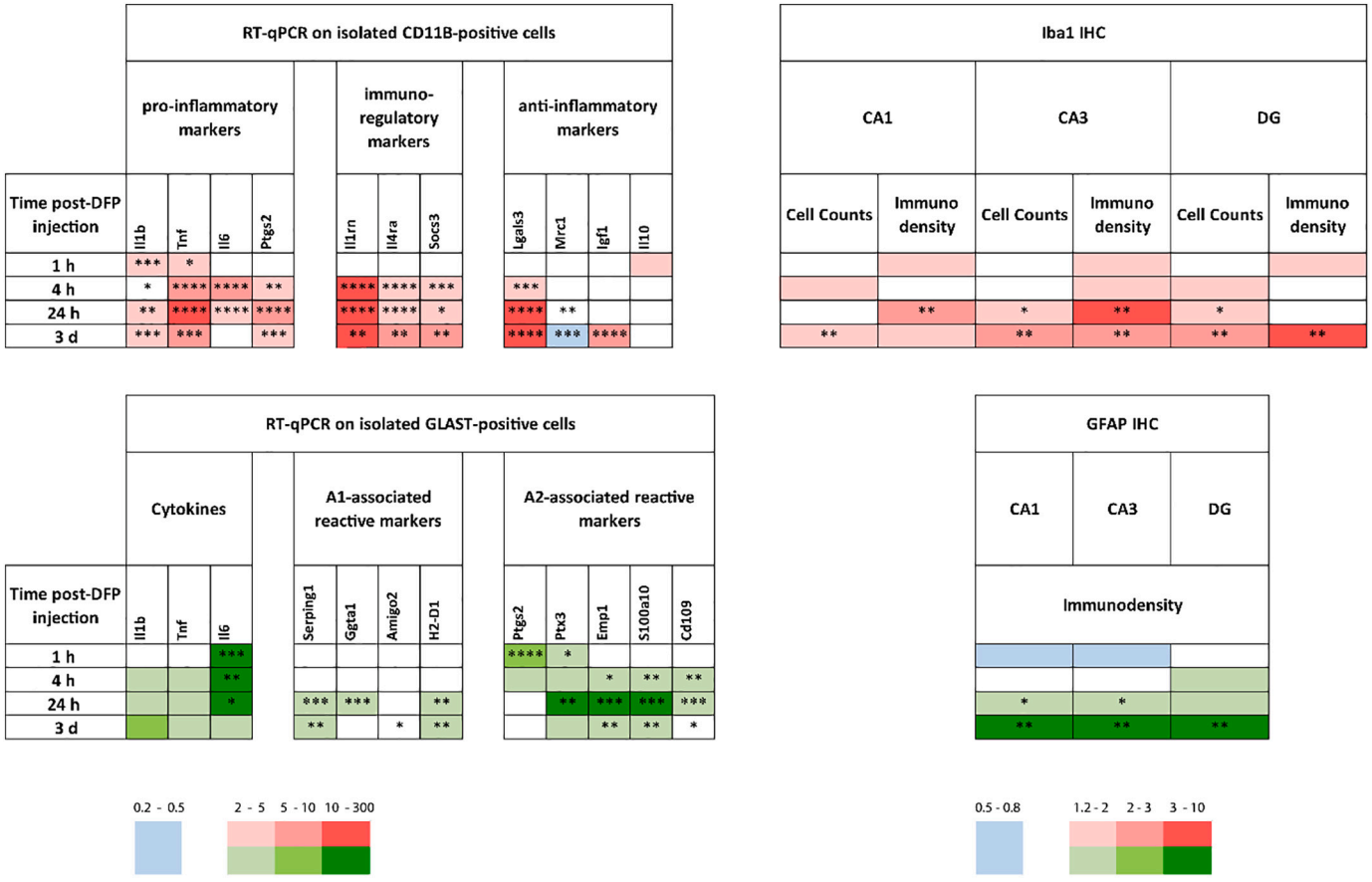

Lgals3 knock-out mice presented a small reduction of cell death in the cortex and no difference in the hippocampus 3 days after pilocarpine injection compared to WT mice; suggesting that, after SE, Galectin-3's protective role is more marginal (Bischoff et al., 2012). Meanwhile, in GLAST-positive isolated cells, while A2-specific markers were maintained, A1-specific markers appeared up-regulated for the first time after DFP exposure. The role of neurotoxic astrogliosis in neurodegeneration has been demonstrated, and different mechanisms have been identified, such as, reduced glutamate clearance, adenosine cycle modifications, increased Ca^{2+} signaling, and BBB dysfunction (Noebels et al., 2012).

Finally, 3 days after DFP injection, we observed a significant increase in Iba1-positive cell number in all hippocampal regions. This increase was already noticeable at 24 h but increased with time (Table 1). In a SE model induced by icv infusion of KA, Feng and colleagues observed microglial proliferation and macrophage infiltration at both 24 h and 3 days SE (Feng et al., 2019). As the Iba1 marker does not permit differentiation of microglial and infiltrated macrophages, we cannot state if the increase in Iba1-positive cells observed at 24 h and 3 days are due to microglia migration, proliferation, or macrophage infiltration. Further work is needed to address this issue in our model. At this time point, in the pilocarpine SE model, pro-inflammatory (M1-like) and anti-inflammatory microglial phenotypes (M2a-like) have been observed in the forebrain (Benson et al., 2015). However, in a SE model induced by intrahippocampal KA, the anti-inflammatory phenotype was not observed at the same time point, showing that model specificity exists (Benson et al., 2015).

5. Conclusions

Our work identified sequential microglial and astrocytic phenotype activation. Given the very early neuroinflammatory modifications observed, targeting these modifications could be a beneficial strategy for

the treatment of refractory SE and its cerebral consequences. This type of intervention should be provided very early in the course of the SE. Further comprehensive study of A2 reactive astrocytes role in SE is nevertheless needed. An adapted treatment paradigm in order to address specific phases of neuroinflammation could increase therapeutic impact.

Ethics approval and consent to participate

A statement on ethics for the experiments involving animals is included in the manuscript.

Consent for publication

Not applicable

Authors' information

Not applicable

Availability of data and materials

The datasets used and/or analyzed during the current study are available from the corresponding author on reasonable request.

Funding

This work was supported by the French Ministry of Armed Forces: Direction Générale de l'Armement (DGA) and Service de Santé des Armées (SSA). Funding sources had no involvement in study design, collection, analysis or interpretation of data, or decision to publish.

Authors' contributions

C.M, J.E, N·D performed the experiments, the analysis and designed the figures. R.H.A and A.I. helped carry out the experiments. M.O performed digital image processing and helped to design the figures. N.D. developed the study design, supervised the project and wrote the manuscript. S.A., N.S·Y, X.B, F·N, G.D contributed to the final manuscript.

Declaration of Competing Interest

The authors declare that they have no competing interests.

Acknowledgments

This work used the imagery platform of IRBA supported by the Service de Santé des Armées. We particularly thank Mr. X. Butigieg for technical support and Mr. J. Kononchik for relevant comments and language editing during the preparation of this manuscript.

Appendix A. Supplementary data

Supplementary data to this article can be found online at https://doi.org/10.1016/j.nbd.2021.105276.

References

Akin, D., Ravizza, T., Maroso, M., Carcak, N., Eryigit, T., Vanzulli, I., et al., 2011. IL-1β is induced in reactive astrocytes in the somatosensory cortex of rats with genetic absence epilepsy at the onset of spike-and-wave discharges, and contributes to their occurrence. Neurobiol. Dis. 44, 259–269.

Aronica, E., Crino, P.B., 2011. Inflammation in epilepsy: clinical observations. Epilepsia. 52 (Suppl. 3), 26–32.

Aronica, E., Ravizza, T., Zurolo, E., Vezzani, A., 2012. Astrocyte immune responses in epilepsy. Glia. 60, 1258–1268.

Auvin, S., Dupuis, N., 2014. Outcome of status epilepticus. What do we learn from animal data? Epileptic Disord. (16 Spec No 1), S37–S43. https://doi.org/10.1684/epd.2014.0670.

Baille, V., Clarke, P.G.H., Brochier, G., Dorandeu, F., Verna, J.-M., Four, E., et al., 2005. Soman-induced convulsions: the neuropathology revisited. Toxicology. 215, 1–24.

Balosso, S., Maroso, M., Sanchez-Alavez, M., Ravizza, T., Frasca, A., Bartfai, T., et al., 2008. A novel non-transcriptional pathway mediates the proconvulsive effects of interleukin-1beta. Brain. 131, 3256–3265.

Bankstahl, J.P., Löscher, W., 2008. Resistance to antiepileptic drugs and expression of P-glycoprotein in two rat models of status epilepticus. Epilepsy Res. 82, 70–85.

Benson, M.J., Manzanero, S., Borges, K., 2015. Complex alterations in microglial M1/M2 markers during the development of epilepsy in two mouse models. Epilepsia. 56, 895–905.

Bischoff, V., Deogracias, R., Poirier, F., Barde, Y.-A., 2012. Seizure-induced neuronal death is suppressed in the absence of the endogenous lectin Galectin-1. J. Neurosci. 32, 15590–15600.

Chhor, V., Le Charpentier, T., Lebon, S., Oré, M.-V., Celador, I.L., Josserand, J., et al., 2013. Characterization of phenotype markers and neuronotoxic potential of polarised primary microglia in vitro. Brain Behav. Immun. 32, 70–85.

Chu, X., Cao, L., Yu, Z., Xin, D., Li, T., Ma, W., et al., 2019. Hydrogen-rich saline promotes microglia M2 polarization and complement-mediated synapse loss to restore behavioral deficits following hypoxia-ischemic in neonatal mice via AMPK activation. J. Neuroinflammation 16, 104.

Cockram, T.O.J., Puigdellívol, M., Brown, G.C., 2019. Calreticulin and galectin-3 opsonise Bacteria for phagocytosis by microglia. Front. Immunol. 10, 2647.

Colton, C.A., 2009. Heterogeneity of microglial activation in the innate immune response in the brain. J. NeuroImmune Pharmacol. 4, 399–418.

de Araujo, Furtado M., Rossetti, F., Chanda, S., Yourick, D., 2012. Exposure to nerve agents: from status epilepticus to neuroinflammation, brain damage, neurogenesis and epilepsy. Neurotoxicology. 33, 1476–1490.

Deshpande, L.S., Blair, R.E., Huang, B.A., Phillips, K.F., DeLorenzo, R.J., 2016. Pharmacological blockade of the calcium plateau provides neuroprotection following organophosphate paraoxon induced status epilepticus in rats. Neurotoxicol. Teratol. 56, 81–86.

Dhir, A., Bruun, D.A., Guignet, M., Tsai, Y.-H., González, E., Calsbeek, J., et al., 2020. Allopregnanolone and perampanel as adjuncts to midazolam for treating diisopropylfluorophosphate-induced status epilepticus in rats. Ann. N. Y. Acad. Sci. 1480, 183–206.

Enderlin, J., Igert, A., Auvin, S., Nachon, F., Dal Bo, G., Dupuis, N., 2020. Characterization of organophosphate-induced brain injuries in a convulsive mouse model of diisopropylfluorophosphate exposure. Epilepsia. 61, e54–e59.

Feng, L., Murugan, M., Bosco, D.B., Liu, Y., Peng, J., Worrell, G.A., et al., 2019. Microglial proliferation and monocyte infiltration contribute to microgliosis following status epilepticus. Glia. 67, 1434–1448.

Ferrara-Bowens, T.M., Chandler, J.K., Guignet, M.A., Irwin, J.F., Laitipaya, K., Palmer, D. D., et al., 2017. Neuropathological and behavioral sequelae in IL-1R1 and IL-1Ra gene knockout mice after soman (GD) exposure. Neurotoxicology. 63, 43–56.

Flannery, B.M., Bruun, D.A., Rowland, D.J., Banks, C.N., Austin, A.T., Kukis, D.L., et al., 2016. Persistent neuroinflammation and cognitive impairment in a rat model of acute diisopropylfluorophosphate intoxication. J. Neuroinflam. [Internet]. 13 [cited 2020 Dec 7]. Available from: https://www.ncbi.nlm.nih.gov/pmc/articles/PMC5062885/.

Guignet, M., Dhakal, K., Flannery, B.M., Hobson, B.A., Zolkowska, D., Dhir, A., et al., 2020. Persistent behavior deficits, neuroinflammation, and oxidative stress in a rat model of acute organophosphate intoxication. Neurobiol. Dis. 133, 104431.

Hamilton, S.E., Loose, M.D., Qi, M., Levey, A.I., Hille, B., McKnight, G.S., et al., 1997. Disruption of the m1 receptor gene ablates muscarinic receptor-dependent M current regulation and seizure activity in mice. Proc. Natl. Acad. Sci. U. S. A. 94, 13311–13316.

Iori, V., Iyer, A.M., Ravizza, T., Beltrame, L., Paracchini, L., Marchini, S., et al., 2017. Blockade of the IL-1R1/TLR4 pathway mediates disease-modification therapeutic effects in a model of acquired epilepsy. Neurobiol. Dis. 99, 12–23.

Johnson, E.A., Kan, R.K., 2010. The acute phase response and soman-induced status epilepticus: temporal, regional and cellular changes in rat brain cytokine concentrations. J. Neuroinflammation 7, 40.

Kadriu, B., Guidotti, A., Costa, E., Auta, J., 2009. Imidazenil, a non-sedating anticonvulsant benzodiazepine, is more potent than diazepam in protecting against DFP-induced seizures and neuronal damage. Toxicology. 256, 164–174.

Kong, W., Hooper, K.M., Ganea, D., 2016. The natural dual cyclooxygenase and 5-lipoxygenase inhibitor flavocoxid is protective in EAE through effects on Th1/Th17 differentiation and macrophage/microglia activation. Brain Behav. Immun. 53, 59–71.

Kuruba, R., Wu, X., Reddy, D.S., 1864. Benzodiazepine-refractory status epilepticus, neuroinflammation, and interneuron neurodegeneration after acute organophosphate intoxication. Biochim. Biophys. Acta Mol. basis Dis. 2018, 2845–2858.

Lalancette-Hébert, M., Swarup, V., Beaulieu, J.M., Bohacek, I., Abdelhamid, E., Weng, Y. C., et al., 2012. Galectin-3 is required for resident microglia activation and proliferation in response to ischemic injury. J. Neurosci. 32, 10383–10395.

Levy, N., Milikovsky, D.Z., Baranauskas, G., Vinogradov, E., David, Y., Ketzef, M., et al., 2015. Differential TGF-β signaling in glial subsets underlies IL-6-mediated epileptogenesis in mice. J. Immunol. 195, 1713–1722.

Li, T., Zhai, X., Jiang, J., Song, X., Han, W., Ma, J., et al., 1657. Intraperitoneal injection of IL-4/IFN-γ modulates the proportions of microglial phenotypes and improves epilepsy outcomes in a pilocarpine model of acquired epilepsy. Brain Res. 2017, 120–129.

Li, Y., Lein, P.J., Liu, C., Bruun, D.A., Tewolde, T., Ford, G., et al., 2011. Spatiotemporal pattern of neuronal injury induced by DFP in rats: a model for delayed neuronal cell death following acute OP intoxication. Toxicol. Appl. Pharmacol. 253, 261–269.
Li, Y., Lein, P.J., Ford, G.D., Liu, C., Stovall, K.C., White, T.E., et al., 2015. Neuregulin-1 inhibits neuroinflammatory responses in a rat model of organophosphate-nerve agent-induced delayed neuronal injury. J. Neuroinflammation 12, 64.
Liddelow, S.A., Guttenplan, K.A., Clarke, L.E., Bennett, F.C., Bohlen, C.J., Schirmer, L., et al., 2017a. Neurotoxic reactive astrocytes are induced by activated microglia. Nature. 541, 481–487.
Liu, C., Li, Y., Lein, P.J., Ford, B.D., 2012. Spatiotemporal patterns of GFAP upregulation in rat brain following acute intoxication with diisopropylfluorophosphate (DFP). Curr. Neurobiol. 3, 90–97.
Liu, J.-T., Wu, S.-X., Zhang, H., Kuang, F., 2018. Inhibition of MyD88 signaling skews microglia/macrophage polarization and attenuates neuronal apoptosis in the hippocampus after status epilepticus in mice. Neurotherapeutics. 15, 1093–1111.
Maroso, M., Balosso, S., Ravizza, T., Liu, J., Aronica, E., Iyer, A.M., et al., 2010. Toll-like receptor 4 and high-mobility group box-1 are involved in ictogenesis and can be targeted to reduce seizures. Nat. Med. 16, 413–419.
Mazarati, A.M., Baldwin, R.A., Sankar, R., Wasterlain, C.G., 1998. Time-dependent decrease in the effectiveness of antiepileptic drugs during the course of self-sustaining status epilepticus. Brain Res. 814, 179–185.
McDonough, J.H., Shih, T.M., 1997. Neuropharmacological mechanisms of nerve agent-induced seizure and neuropathology. Neurosci. Biobehav. Rev. 21, 559–579.
McDonough, J.H., McMonagle, J.D., Shih, T.-M., 2010. Time-dependent reduction in the anticonvulsant effectiveness of diazepam against soman-induced seizures in Guinea pigs. Drug Chem. Toxicol. 33, 279–283.
Noe, F.M., Polascheck, N., Frigerio, F., Bankstahl, M., Ravizza, T., Marchini, S., et al., 2013. Pharmacological blockade of IL-1β/IL-1 receptor type 1 axis during epileptogenesis provides neuroprotection in two rat models of temporal lobe epilepsy. Neurobiol. Dis. 59, 183–193.
Noebels, J.L., Avoli, M., Rogawski, M.A., Olsen, R.W., Delgado-Escueta, A.V., 2012. Jasper's Basic Mechanisms of the Epilepsies [Internet], 4th ed. National Center for Biotechnology Information (US), Bethesda (MD) [cited 2020 Jul 27]. Available from: http://www.ncbi.nlm.nih.gov/books/NBK50785/.
Prinz, M., Priller, J., Sisodia, S.S., Ransohoff, R.M., 2011. Heterogeneity of CNS myeloid cells and their roles in neurodegeneration. Nat. Neurosci. 14, 1227–1235.
Qiao, D., Seidler, F.J., Abreu-Villaça, Y., Tate, C.A., Cousins, M.M., Slotkin, T.A., 2004. Chlorpyrifos exposure during neurulation: cholinergic synaptic dysfunction and cellular alterations in brain regions at adolescence and adulthood. Brain Res. Dev. Brain Res. 148, 43–52.
Ransohoff, R.M., 2016. A polarizing question: do M1 and M2 microglia exist? Nat. Neurosci. 19, 987–991.
Ravizza, T., Gagliardi, B., Noé, F., Boer, K., Aronica, E., Vezzani, A., 2008a. Innate and adaptive immunity during epileptogenesis and spontaneous seizures: evidence from experimental models and human temporal lobe epilepsy. Neurobiol. Dis. 29, 142–160.
Ravizza, T., Noé, F., Zardoni, D., Vaghi, V., Sifringer, M., Vezzani, A., 2008b. Interleukin converting enzyme inhibition impairs kindling epileptogenesis in rats by blocking astrocytic IL-1beta production. Neurobiol. Dis. 31, 327–333.
Rideau Batista Novais, A., Pham, H., Van de Looij, Y., Bernal, M., Mairesse, J., Zana-Taieb, E., et al., 2016. Transcriptomic regulations in oligodendroglial and microglial cells related to brain damage following fetal growth restriction. Glia. 64, 2306–2320.
Rojas, A., Ganesh, T., Lelutiu, N., Gueorguieva, P., Dingledine, R., 2015. Inhibition of the prostaglandin EP2 receptor is neuroprotective and accelerates functional recovery in a rat model of organophosphorus induced status epilepticus. Neuropharmacology. 93, 15–27.
Shiow, L.R., Favrais, G., Schirmer, L., Schang, A.-L., Cipriani, S., Andres, C., et al., 2017. Reactive astrocyte COX2-PGE2 production inhibits oligodendrocyte maturation in neonatal white matter injury. Glia. 65, 2024–2037.
Shrot, S., Ramaty, E., Biala, Y., Bar-Klein, G., Daninos, M., Kamintsky, L., et al., 2014. Prevention of organophosphate-induced chronic epilepsy by early benzodiazepine treatment. Toxicology. 323, 19–25.
Sisó, S., Hobson, B.A., Harvey, D.J., Bruun, D.A., Rowland, D.J., Garbow, J.R., et al., 2017. Editor's highlight: spatiotemporal progression and remission of lesions in the rat brain following acute intoxication with diisopropylfluorophosphate. Toxicol. Sci. 157, 330–341.
Sofroniew, M.V., Vinters, H.V., 2010. Astrocytes: biology and pathology. Acta Neuropathol. 119, 7–35.
Steinhäuser, C., Seifert, G., 2012. Astrocyte dysfunction in epilepsy. In: Noebels, J.L., Avoli, M., Rogawski, M.A., Olsen, R.W., Delgado-Escueta, A.V. (Eds.), Jasper's Basic Mechanisms of the Epilepsies [Internet], 4th ed. National Center for Biotechnology Information (US), Bethesda (MD) [cited 2020 Jul 30]. Available from: http://www.ncbi.nlm.nih.gov/books/NBK98180/.
Todorovic, M.S., Cowan, M.L., Balint, C.A., Sun, C., Kapur, J., 2012. Characterization of status epilepticus induced by two organophosphates in rats. Epilepsy Res. 101, 268–276.
van Vliet, E.A., Aronica, E., Vezzani, A., Ravizza, T., 2018. Review: Neuroinflammatory pathways as treatment targets and biomarker candidates in epilepsy: emerging evidence from preclinical and clinical studies. Neuropathol. Appl. Neurobiol. 44, 91–111.
Vezzani, A., Moneta, D., Conti, M., Richichi, C., Ravizza, T., De Luigi, A., et al., 2000. Powerful anticonvulsant action of IL-1 receptor antagonist on intracerebral injection and astrocytic overexpression in mice. Proc. Natl. Acad. Sci. U. S. A. 97, 11534–11539.
Vezzani, A., Ravizza, T., Balosso, S., Aronica, E., 2008. Glia as a source of cytokines: implications for neuronal excitability and survival. Epilepsia. 49 (Suppl. 2), 24–32.
Vezzani, A., Balosso, S., Maroso, M., Zardoni, D., Noé, F., Ravizza, T., 2010. ICE/caspase 1 inhibitors and IL-1beta receptor antagonists as potential therapeutics in epilepsy. Curr. Opin. Investig. Drugs 11, 43–50.
Vezzani, A., Maroso, M., Balosso, S., Sanchez, M.-A., Bartfai, T., 2011. IL-1 receptor/toll-like receptor signaling in infection, inflammation, stress and neurodegeneration couples hyperexcitability and seizures. Brain Behav. Immun. 25, 1281–1289.
Vezzani, A., Balosso, S., Ravizza, T., 2019. Neuroinflammatory pathways as treatment targets and biomarkers in epilepsy. Nat. Rev. Neurol. 15, 459–472.
Vinet, J., Vainchtein, I.D., Spano, C., Giordano, C., Bordini, D., Curia, G., et al., 2016. Microglia are less pro-inflammatory than myeloid infiltrates in the hippocampus of mice exposed to status epilepticus. Glia. 64, 1350–1362.
Wu, X., Kuruba, R., Reddy, D.S., 2018. Midazolam-resistant seizures and brain injury after acute intoxication of diisopropylfluorophosphate, an organophosphate pesticide and surrogate for nerve agents. J. Pharmacol. Exp. Ther. 367, 302–321.
Xu, Z.-H., Wang, Y., Tao, A.-F., Yu, J., Wang, X.-Y., Zu, Y.-Y., et al., 2016. Interleukin-1 receptor is a target for adjunctive control of diazepam-refractory status epilepticus in mice. Neuroscience. 328, 22–29.
Xu, X., Gao, W., Cheng, S., Yin, D., Li, F., Wu, Y., et al., 2017. Anti-inflammatory and immunomodulatory mechanisms of atorvastatin in a murine model of traumatic brain injury. J. Neuroinflammation 14, 167.
Yuan, Y., Wu, C., Ling, E.-A., 2019. Heterogeneity of microglia phenotypes: developmental, functional and some therapeutic considerations. Curr. Pharm. Des. 25, 2375–2393.
Zamanian, J.L., Xu, L., Foo, L.C., Nouri, N., Zhou, L., Giffard, R.G., et al., 2012. Genomic analysis of reactive astrogliosis. J. Neurosci. 32, 6391–6410.